Desalination and Water Treatment
www.deswater.com
doi: 10.5004/dwt.2023.30087

314 (2023) 219–230
December

Degradation of Eriochrome Black T by heterogeneous electro-Fenton: a comparison study

Hadjer Belbel[a], Rachid Delimi[a], Zahia Benredjem[a,*], Karima Barbari[b], Laouar Rabah[c]

[a]*Laboratory of Water Treatment and Valorization of Industrial Wastes, Department of Chemistry, Faculty of Sciences, Badji Mokhtar-Annaba University, Annaba, Bp 12, 23000, Algeria, emails: z.benredjem@gmail.com/ zahia.benredjem@univ-annaba.dz (Z. Benredjem), belbelhadjer@gmail.com (H. Belbel), rachid.delimi@univ-annaba.dz (R. Delimi)*
[b]*Environmental Research Center, Campus Sidi Amar Badji Mokhtar-Annaba University Annaba, Algeria, email: karima.barbari@hotmail.fr (K. Barbari)*
[c]*Department of Geology, Badji Mokhtar-Annaba University and Laboratory of Geodynamics, Engineering Geology and Plantology, FSTGAT, USTHB, Algiers, email: rabahlaouar@yahoo.fr (R. Laouar)*

Received 26 April 2023; Accepted 12 October 2023

ABSTRACT

The use of natural catalysts in various processes, including the electro-Fenton (EF) process, is a topic of interest in current research and development. Natural catalysts are being explored as potential alternatives to conventional catalysts due to their advantages such as sustainability, low-cost, and environmental compatibility. It is worth noting that the application of natural catalysts in the EF process is an active area of ongoing research, and their full-scale implementation may still require further development and optimization. That is why in our work, we chose to use hematite and pyrite as natural catalysts in the degradation of the black azo dye Eriochrome Black T (EBT) by EF process. Color and chemical oxygen demand (COD) removal efficiencies were compared with those obtained with the conventional catalyst ($FeSO_4$). The pyrite-EF process followed a pseudo-second-order and was found to be more efficient than the hematite-EF process due to the self-adjustment of its pH, it gave slightly lower color (90.30%) and COD (89.20%) removal rates than those obtained with the conventional catalyst (93.05% and 92.06%) after 60 min of treatment. The morphology, chemical composition and crystal structure of hematite and pyrite samples were identified by scanning electron microscopy, X-ray fluorescence and X-ray diffraction analyses. Furthermore, the study of some operating parameters effects allowed determining the optimal conditions for treatment of the Eriochrome Black T solution: 0.03 $g{\cdot}L^{-1}$ (pyrite dose), 8×10^{-3} M (supporting electrolyte concentration) and 15 $mA{\cdot}cm^{-2}$ (current density). The pyrite-EF process showed similar behavior to that of $FeSO_4$-EF with a low energy consumption. Therefore, EBT can be efficiently removed electrochemically using natural pyrite as an eco-friendly catalyst.

Keywords: Persistent organic pollutants; Wastewater treatment; Advanced oxidation processes; Electro-Fenton; Hematite; Pyrite

1. Introduction

The global dye industry has experienced significant growth over the last few years, driven by increasing demand from various sectors such as textiles, printing, leather, paper, and plastics [1]. The industry encompasses both natural and synthetic dye production, with synthetic dyes being more predominant due to their wide range of applications and cost-effectiveness [2]. The textile industry is one of the primary drivers of dye consumption due to its extensive use of dyes for fabric coloring. Dyes, particularly synthetic azo dyes can pose risks to humans by causing

* Corresponding author.

allergic reactions, endocrine disruption and carcinogenicity [3–6]. In the environment and water sources dye wastewater, if not properly treated, can be discharged into water bodies, leading to the pollution of both surface and ground waters [7]. Dyes can impart intense coloration to water bodies, reducing light penetration and disrupting aquatic ecosystems. Some dyes and their degradation products have the toxic potential to accumulate in the tissues of aquatic organisms and thus enter the food chain. This can result in the increase of dye-related risks as higher trophic levels consume contaminated organisms [8,9].

To mitigate the risks associated with dyes, several standards, regulations and measures can be followed, including implementing proper wastewater treatment technologies to remove dyes and minimize their environmental impact before discharge. Classical methods for water treatment refer to the traditional and widely used techniques that have been employed for decades. These methods have many advantages but also have multiple limitations; they can either partially remove the pollution or displace it, creating a new problem for the management of dye-laden waste. For example, filtration can improve water clarity but alone may not be sufficient for the removal of dissolved organic compounds, nutrients, or certain pathogens also regular maintenance and cleaning of filters are necessary and high-pressure drop across filters can lead to increased energy consumption [10]. Coagulation and flocculation effectively removes suspended particles, colloids, and turbidity, the process is relatively simple and widely applicable but may require the use of chemical coagulants, such as aluminum or iron salts, which can contribute to sludge generation and increased chemical usage [11]. Disinfection kills or inactivates a wide range of microorganisms, including bacteria, viruses, and parasites; however, it can produce disinfection by-products, some of which may be harmful [12]. Adsorption effectively removes dissolved organic compounds, taste, odor, and some chemicals; in revenge, it requires regular replacement or regeneration of the adsorbent material [13]. It is important to note that the selection and combination of water treatment methods depend on the specific water quality characteristics, target contaminants, regulatory requirements, and the desired treated water quality. Often, a combination of multiple treatment processes or the use of advanced oxidation processes (AOPs) are employed in water treatment to achieve comprehensive and efficient water purification [14–17].

AOPs are a set of treatment methods that utilize highly reactive hydroxyl radicals (•OH) which are very strong oxidants (E = 2.8 V vs. Standard Hydrogen Electrode, SHE) [18] to degrade and remove organic pollutants from water and wastewater, these radicals attack most organic molecules with rate constants usually in the order of 10^6–10^9 L·mol^{-1}·s^{-1} [19]. AOPs involve the generation of hydroxyl radicals through various mechanisms, including chemical reactions, photocatalysis, or electrochemical reactions. They have gained significant attention due to their ability to effectively treat recalcitrant and persistent organic compounds. The electro-Fenton (EF), one of the highly used AOPs is based on Fenton's reagent which is a reaction between Fe^{2+} and H_2O_2 Eq. (1) [20].

$$Fe^{2+} + H_2O_2 \rightarrow Fe^{3+} + OH^- + {}^{\bullet}OH \quad (1)$$

EF process holds significant importance for the treatment of various pollutants, including dyes [21], pharmaceuticals [22–24], pesticides [25] and other aromatic compounds that are resistant to conventional treatment methods in wastewater treatment due to its unique capabilities to transform them into benign compounds like carbon dioxide, water and inorganic ions. It can be applied to treat diverse types of wastewater, including industrial effluents, municipal wastewater, and contaminated groundwater.

Despite the encouraging results obtained in numerous studies on the EF process, the latter remains relatively expensive. Ongoing studies aim to enhance process efficiency, reduce energy consumption, and address challenges related to byproduct formation and catalyst regeneration. This can be improved by using natural catalysts, derived from renewable resources that are being investigated as alternatives to conventional catalysts. These natural catalysts can offer several benefits such as cost-effectiveness, as they can be obtained from readily available sources, reducing the reliance on expensive or rare metals. They have low toxicity and are more environmentally friendly compared to conventional catalysts, which may contain hazardous or polluting substances.

While the use of natural catalysts in the EF process is still a relatively new area of research, there have been promising findings to enhance the efficiency and effectiveness of the EF process. Researchers are investigating various alternatives such as the use of industrial by-products [26] or natural minerals (hematite, magnetite, goethite, pyrite, etc.) as catalysts in the EF process [27–36]. However, few studies report a comparison of the efficiency of these natural catalysts with the commonly used catalyst, iron sulphate.

That is why in our study, we chose to replace the conventional catalyst ($FeSO_4$) with natural minerals hematite and pyrite, the Eriochrome Black T (EBT) removal efficiencies were compared with those of $FeSO_4$-EF. Scanning electron microscopy (SEM), X-ray fluorescence and X-ray diffraction (XRD) techniques have been applied to characterize natural catalysts. Energy consumption and the effect of certain operating parameters on the removal efficiency of the process were investigated.

2. Materials and methods

2.1. Chemicals

The dyestuff solution was prepared dissolving 100 mg·L^{-1} of Eriochrome Black T (provided by Sigma-Aldrich) in bi-distilled water. Sodium sulfate Na_2SO_4 and ferric sulfate $FeSO_4{\cdot}7H_2O$, supplied by Sigma-Aldrich, were used as supporting electrolyte and catalyst, respectively. Other reagents used for chemical oxygen demand (COD) determination including potassium dichromate ($K_2Cr_2O_7$), mercuric sulfate ($HgSO_4$), sulfuric acid (H_2SO_4), silver sulfate (Ag_2SO_4) were purchased from Merck. The natural hematite and pyrite used in this work as catalysts come from the Anini (Sétif, Algeria) and Ain Barbar (Annaba, Algeria) mountains, respectively. The particle size of the two natural catalysts used in this study is approximately 65 μm. The carbon felt was purchased from Carbone Lorraine and the pharmaceutical grade 316 L stainless steel plates were supplied by MD Metal Tunisia.

2.2. Electrochemical process

The experimental set-up (Fig. 1) employed in the EBT degradation by electro-Fenton essentially comprises a power supply (Voltcraft PS 405 Pro) and an undivided and open electrochemical reactor, in the form of a cylindrical cell. Electrolysis in galvanostatic mode of solution (200 mL) at room temperature was performed between a carbon felt cathode and a stainless-steel anode with an effective geometric area of 31.5 cm^2. The current intensity was monitored with a multimeter (Metrix MX52). Experiments were conducted in batch mode and the solution was continuously mixed with a magnetic stirrer. Oxygen was supplied to the solution by bubbling (0.2 $L \cdot min^{-1}$) compressed and purified air. Before starting the electrolysis, a well-defined amount of catalyst (pyrite, hematite ore or ferrous sulfate) has been added to the EBT solution containing Na_2SO_4 as the supporting electrolyte and shortly after the pH was adjusted to 3 with 0.1 M of H_2SO_4. At given time intervals, samples of 5 mL were collected from the electrochemical reactor and Eriochrome Black T concentration and COD were analyzed immediately. All the results were expressed as an average of three replicates.

2.3. Analytical procedures

Color removal was monitored by measuring absorbance decrease at a 540 nm wavelength using a spectrophotometer (SPECORD 200). pH was measured using a HANNA Instruments 211 pH-meter. The color removal of Eriochrome Black T was calculated from Eq. (2), where C_0 and C_t are the concentration at initial time and at time t, respectively.

$$\text{Color removal}\ (\%) = \frac{C_0 - C_t}{C_0} \times 100 \quad (2)$$

The limit of detection (LOD) and limit of quantification (LOQ) of the EBT concentration by the spectrophotometric method using the SPECORD 200 spectrophotometer are 2.04 and 6.82 $mg \cdot L^{-1}$, respectively.

Solution mineralization efficiency was monitored by measuring its COD evolution. COD was determined by the dichromate method using a thermoreactor (WTW CR2200) and the spectrophotometer. The method consists on oxidizing the organic matter by an excess of potassium dichromate in concentrated sulfuric acid medium in the presence of silver sulfate (Ag_2SO_4) and mercuric sulfate ($HgSO_4$). The solution obtained is heated during 2 h at 150°C. The absorbance value of the excess dichromate is translated into COD using a calibration curve [37]. The COD removal was calculated according to Eq. (3). Where COD_0 and COD_t are, respectively, the solution COD values at initial and t time of the electrolysis.

$$\text{COD removal}\ (\%) = \frac{COD_0 - COD_t}{COD_0} \times 100 \quad (3)$$

3. Results and discussion

3.1. Characterization of natural catalysts

3.1.1. Scanning electron microscopy

The Thermo Scientific Quattro environmental scanning electron microscope was used to analyze and confirm the surface morphology of the natural catalysts used. SEM images (Fig. 2a) of the pyrite powder show crystals with well-defined contours and a very smooth surface.

However, SEM analysis of the hematite powder in Fig. 2b reveals non-uniform and entangled lamellar crystals of stubby shape with a rough surface. This morphology is characteristic of hematite crystals.

3.1.2. X-ray fluorescence

The results of the X-ray fluorescence analysis of the pyrite and hematite samples are presented in Tables 1

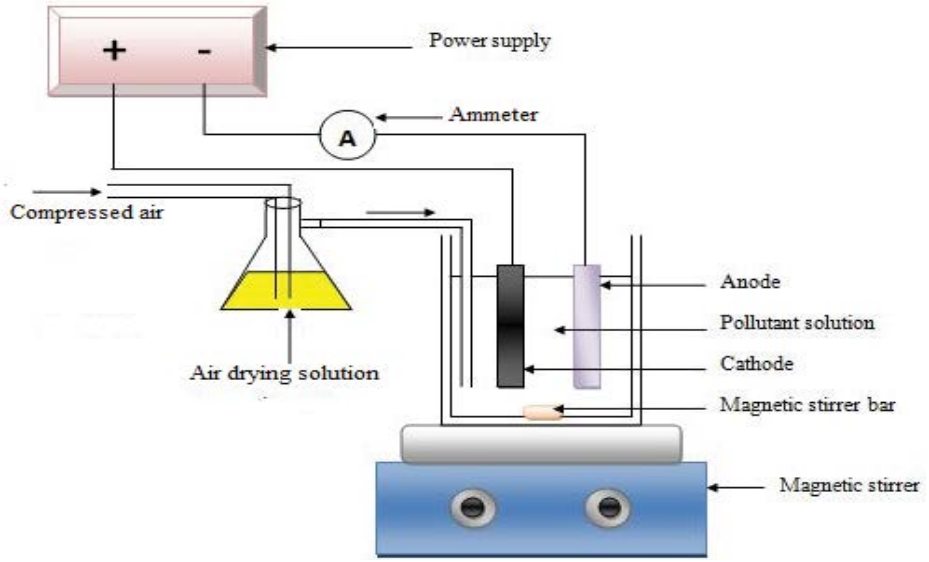

Fig. 1. Schematic diagram of electro-Fenton experimental set-up.

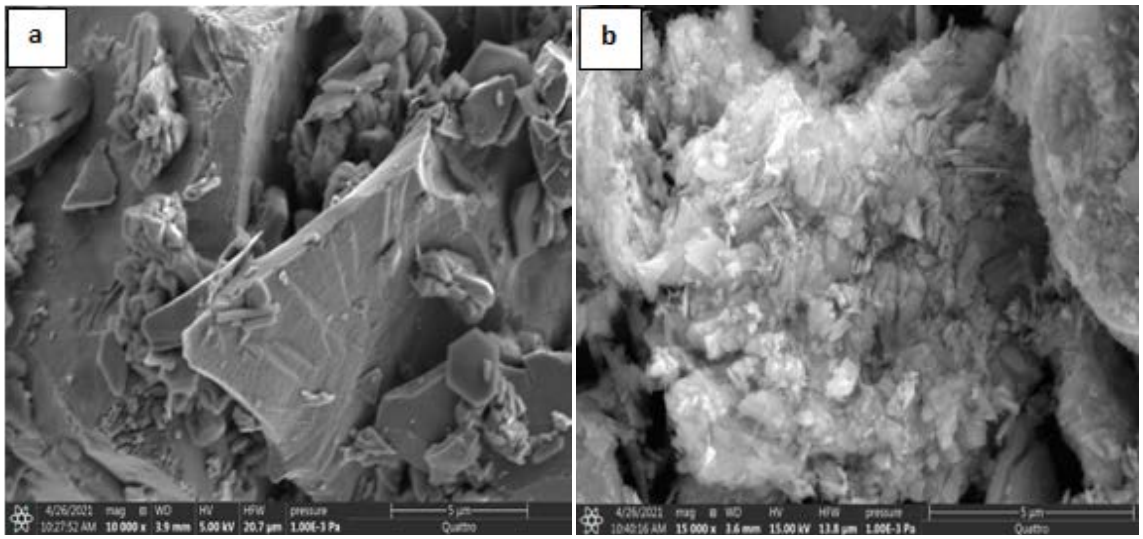

Fig. 2. Scanning electron microscopy images of the natural catalysts (a: pyrite; b: hematite).

Table 1
Chemical composition of pyrite sample analyzed by X-ray fluorescence

Element/compound	wt.%
Fe	53.04
S	36.45
SiO_2	7.31
P_2O_5	0.91
Al_2O_3	0.65
CaO	0.71
PbO	0.55
CoO	0.49
As_2O_3	0.30
WO_3	0.11

Table 2
Chemical composition of hematite samples analyzed by X-ray fluorescence

Compound	wt.%
Fe_2O_3	92.38
Sb_2O_3	2.33
As_2O_3	1.31
SiO_2	1.20
PbO	1.10
Al_2O_3	0.71
P_2O_5	0.42
ZnO	0.41
SO_3	0.15
CuO	0.03

and 2, respectively. The pyrite sample shows weight percentage values of iron of 53.05% and sulfur of 36.45% (Table 1). Compared to the existing ratio between iron and sulfur (Fe/S:56/64) in the pyrite molecule (FeS_2), the weight percentage of Fe is superior to that of S in the pyrite sample. This result means that in addition to pyrite, iron exists in the sample in other compounds. On the other hand, Table 2 reveals that the hematite sample is relatively rich in hematite (92.38%), which corresponds to an iron weight percentage of (64.66%). Finally, it can be noticed that the hematite sample is slightly richer in iron than the pyrite sample.

3.1.3. X-ray diffraction

To characterize the crystal structure of pyrite and hematite powders by XRD we used PANalytical diffractometer Empyrean with CuKα = 1.5418 using software programs DataCollector and HighScore Plus. The peaks intensity and their position in the diffractogram of the pyrite sample presented by Fig. 3 are given in Table 3. The correspondence of the 2θ values of the peaks obtained with those standards of pyrite is evaluated with a score of 50%.

The hematite powder diffractogram presented in Fig. 4 is richer in peaks than that of pyrite. The 2θ values and their intensities of hematite sample are presented in Table 4. The three peaks with 2θ: 21.32, 33.13 and 35.65 indicates the presence of goethite.

3.2. Comparison of EBT degradation efficiencies by electro-Fenton using natural and conventional catalysts

Hematite and pyrite as natural catalysts, and ferrous sulphate, the most commonly used catalyst in EF, were tested in the degradation of Eriochrome Black T by EF. A comparison of the efficiency of the natural catalysts (hematite and pyrite) with that of the conventional catalyst (ferrous sulphate) is shown in Fig. 5a. For all three catalysts the degradation kinetics of EBT follows the order: iron sulphate > pyrite > hematite. It is noticeable that the degradation

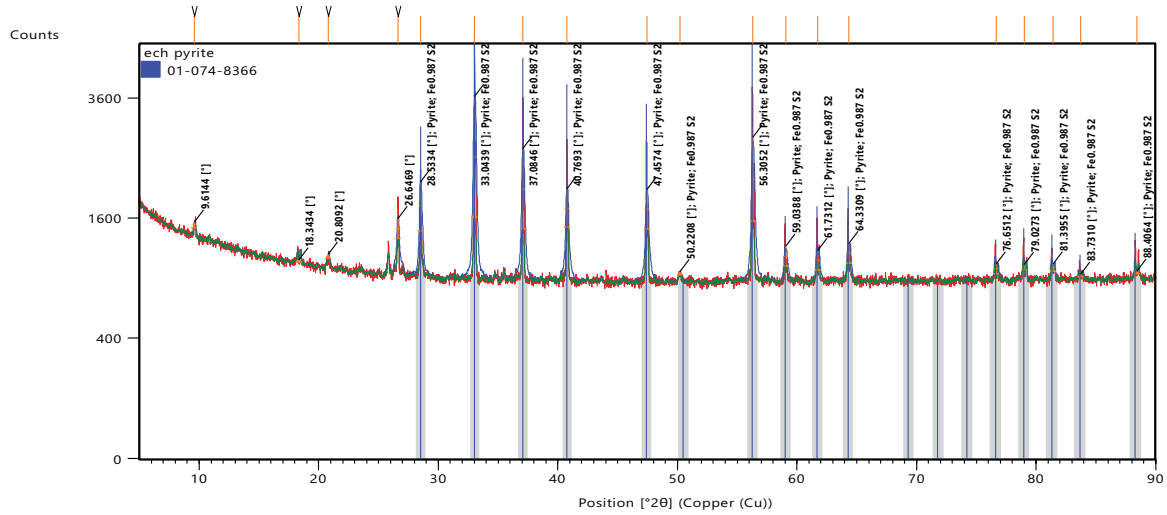

Fig. 3. X-ray diffraction of pyrite.

Table 3
Values of 2θ, the *d*-spacing and the peaks size of the pyrite powder

Pos. (°2θ)	Height (cts)	FWHM Left (°2θ)	*d*-spacing (Å)	Rel. Int. (%)
9.6144	74.70	0.3070	9.19939	3.71
18.3434	23.15	0.4093	4.83669	1.15
20.8092	50.65	0.3070	4.26880	2.52
26.6469	250.82	0.4093	3.34538	12.46
28.5334	683.78	0.3070	3.12835	33.98
33.0439	2,012.57	0.3070	2.71091	100.00
37.0846	1,196.00	0.3070	2.42429	59.43
40.7693	527.12	0.4093	2.21330	26.19
47.4574	549.71	0.4093	1.91582	27.31
50.2208	34.71	0.3070	1.81669	1.72
56.3052	1,298.14	0.3070	1.63396	64.50
59.0388	227.17	0.3070	1.56466	11.29
61.7312	212.89	0.3070	1.50273	10.58
64.3309	222.44	0.3070	1.44813	11.05
76.6512	102.78	0.3070	1.24319	5.11
79.0273	54.23	0.3070	1.21167	2.69
81.3955	72.06	0.3070	1.18229	3.58
83.7310	25.40	0.3070	1.15516	1.26
88.4064	26.35	0.4093	1.10575	1.31

Visible	Ref. code	Score	Compound name	Displ. (°2θ)	Scale fac.	Chem. formula
*	01-074-8366	50	Iron sulfide	0.000	0.895	$Fe_{0.987}S_2$

kinetics obtained with pyrite is slightly lower than that recorded with the conventional catalyst. Indeed, after only 60 min of treatment, the degradation rates obtained with hematite, pyrite and the conventional catalyst are 77.19%, 85.71% and 90.17%, respectively.

On the other hand, the study of the mineralization efficiency of EBT by EF using different catalysts (Fig. 5b) shows a sequence of catalyst efficiency identical to that of Eriochrome Black T degradation. The COD removal rates recorded after 60 min of electrolysis for hematite, pyrite and $FeSO_4$ are 76.13%, 84.01% and 89.73%, respectively. For the mineralization efficiency we also found out that the difference between the removal rates obtained with pyrite and the conventional catalyst is not significant. However, the high efficiency of the pyrite-EF process compared to the hematite-EF process could be attributed to the

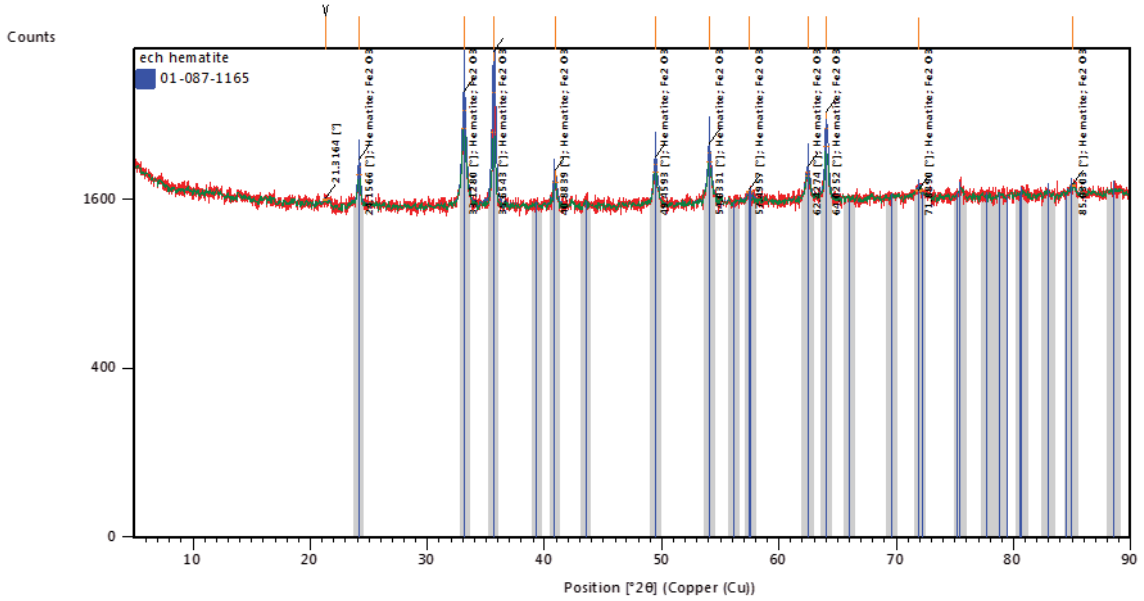

Fig. 4. X-ray diffraction of hematite.

Table 4
Values of 2θ, the *d*-spacing and the peaks size of the hematite powder

Pos. (°2θ)	Height (cts)	FWHM Left (°2θ)	*d*-spacing (Å)	Rel. Int. (%)
21.3164	17.83	0.6140	4.16836	1.76
24.1566	158.33	0.3070	3.68432	15.62
33.1280	455.40	0.3070	2.70422	44.93
35.6543	1,013.68	0.3070	2.51820	100.00
40.8839	124.61	0.4093	2.20735	12.29
49.4593	155.73	0.3070	1.84286	15.36
54.0331	198.06	0.3070	1.69717	19.54
57.4957	36.03	0.6140	1.60293	3.55
62.4274	95.98	0.4093	1.48763	9.47
64.0252	395.26	0.2558	1.45431	38.99
71.8890	11.18	0.8187	1.31335	1.10
85.0303	19.48	0.6140	1.14080	1.92

Visible	Ref. code	Score	Compound name	Displ. (°2θ)	Scale fac.	Chem. formula
*	01-087-1165	13	Iron oxide	0.000	0.376	Fe_2O_3

self-regulation of iron ions in solution in the presence of O_2. This result leads to the conclusion that natural pyrite could be used instead of $FeSO_4$ to effectively degrade the Eriochrome Black T dye by the EF process. That is why we have chosen pyrite as a catalyst in order to carry out experiments on the degradation of EBT by EF.

3.2.1. Effect of different operating parameters on the degradation of EBT using a natural catalyst (pyrite)

In order to optimize the operating conditions for the EBT oxidation by the pyrite- EF process, the effect of certain operating parameters on the process efficiency was investigated.

3.2.2. Effect of pH

Most studies reported that the optimum pH of Fenton process is around 3 [21,38,39]. On the other hand, some studies reported that the use of FeS_2 as a heterogeneous catalyst overcomes the need to adjust the pH value of the solution to about 3 (optimal pH for the Fenton reaction) by self-regulating the pH around 3 by natural pyrite. To verify this, we prepared four solutions of EBT at 50 mg·L^{-1}

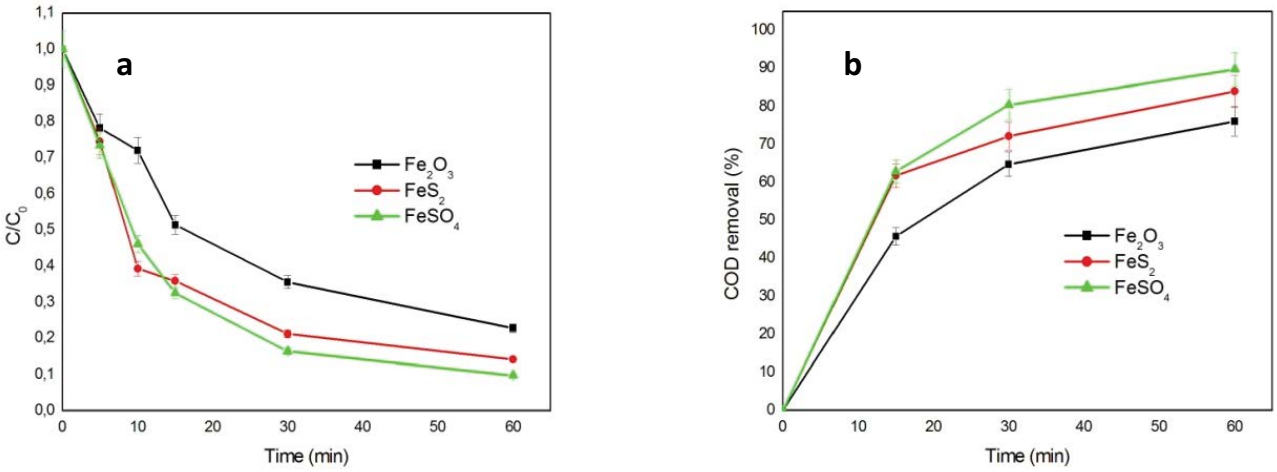

Fig. 5. Kinetics of (a) degradation and (b) mineralization of Eriochrome Black T by electro-Fenton using natural and conventional catalysts ([EBT] = 50 mg·L^{-1}; [$FeSO_4$] = 0.076 g·L^{-1}; [pyrite] = 0.06 g·L^{-1}; [hematite] = 0.08 g·L^{-1}; [Na_2SO_4] = 1.7 × 10^{-2} M; pH = 3; i = 15 mA·cm^{-2}; V = 200 mL).

Table 5
Initial pH of the Eriochrome Black T solution as a function of the dose of natural pyrite

Pyrite dose (g·L^{-1})	0.012	0.03	0.06	0.12
Solution pH	3.1	2.8	2.8	2.7

each containing Na_2SO_4 at 1.7 × 10^{-2} M. To each solution we added a different amount of natural pyrite. After a good stirring of the solution we measured the pH of the solution (Table 5). It was revealed that all four solutions had a pH value close to 3. There was also a slight tendency for the pH to decrease as the dose of natural pyrite increased. Thus, it is concluded that it is not necessary to adjust the pH of the solution to the optimal value (3).

3.2.3. Effect of EBT concentration

The effect of the dye concentration on the degradation efficiency of EBT by heterogeneous electro-Fenton was studied by varying the Eriochrome Black T concentration between 10 and 100 mg·L^{-1}. Fig. 6 shows that for both catalysts (natural pyrite (Fig. 6a); conventional catalyst (Fig. 6b)), the discoloration efficiency of the Eriochrome Black T solution decreases with increasing Eriochrome Black T concentration. Indeed, after 60 min treatment of Eriochrome Black T solutions at concentrations of 10, 25, 50 and 100 mg·L^{-1} by the pyrite-EF process, the discoloration efficiencies recorded are 91.17%, 87.36%, 86.75% and 78.15%, respectively. We noted that increasing the Eriochrome Black T concentration from 10 to 50 mg·L^{-1} does not result in a significant decrease in efficiency. However, for a concentration of 100 mg·L^{-1}, the decrease in the efficiency of the pyrite-EF process is relatively significant. With the conventional catalyst, the same trend of efficiency variation with EBT concentration observed with natural pyrite was recorded. The increase in Eriochrome Black T concentration also influences the efficiency of COD removal. For both catalysts (natural pyrite (Fig. 6c) and conventional catalyst (Fig. 6d)) tested, increasing the initial Eriochrome Black T concentration leads to a decrease in COD removal efficiency. This decrease is slightly more pronounced when the concentration is increased from 50 to 100 mg·L^{-1}. The decrease in discoloration efficiency with increasing Eriochrome Black T concentration was probably due in large part to the decrease in the •OH/Eriochrome Black T ratio with increased Eriochrome Black T concentration and also to the increase in the amount of oxidation products on the electrode surface which prevent contact between Eriochrome Black T molecules and active sites [40]. The same trend was observed with the results of COD removal (Fig. 6c). However, EBT mineralization was found to be slightly more difficult than discoloration. Indeed, for the Eriochrome Black T solutions 10, 25, 50 and 100 mg·L^{-1} and after 15 min of process, the color removal percentages were 61.02%, 60.22%, 62.57% and 57.93%. On the other hand, for the same solutions and the same duration COD removal rates were 47.94%, 50.10%, 59.73% and 54.25%, respectively. Moreover, the comparison between the discoloration (Fig. 6a and b) and mineralization (Fig. 6c and d) efficiencies shows insignificant differences between the efficiencies of pyrite-EF and $FeSO_4$-EF.

3.2.4. Effect of natural catalyst dosage

In order to optimize the dose of pyrite to be introduced into the system, experiments on the degradation of EBT solution by electro-Fenton were carried out for different doses of pyrite Fig. 7a clearly shows that the efficiency of the pyrite-EF process depends on the pyrite dose. First, an increase in discoloration efficiency from 81.23% to 87.50% was observed when the dose of natural catalyst was increased from 0.012 to 0.03 g·L^{-1}, and then beyond the 0.03 g·L^{-1} dose the effect was negative. Indeed, the Eriochrome Black T degradation efficiency recorded for the 0.12 g·L^{-1} dose is equal to 75.24%. For the mineralization of the Eriochrome Black T solution, an identical effect of the pyrite dose on the COD removal efficiency was

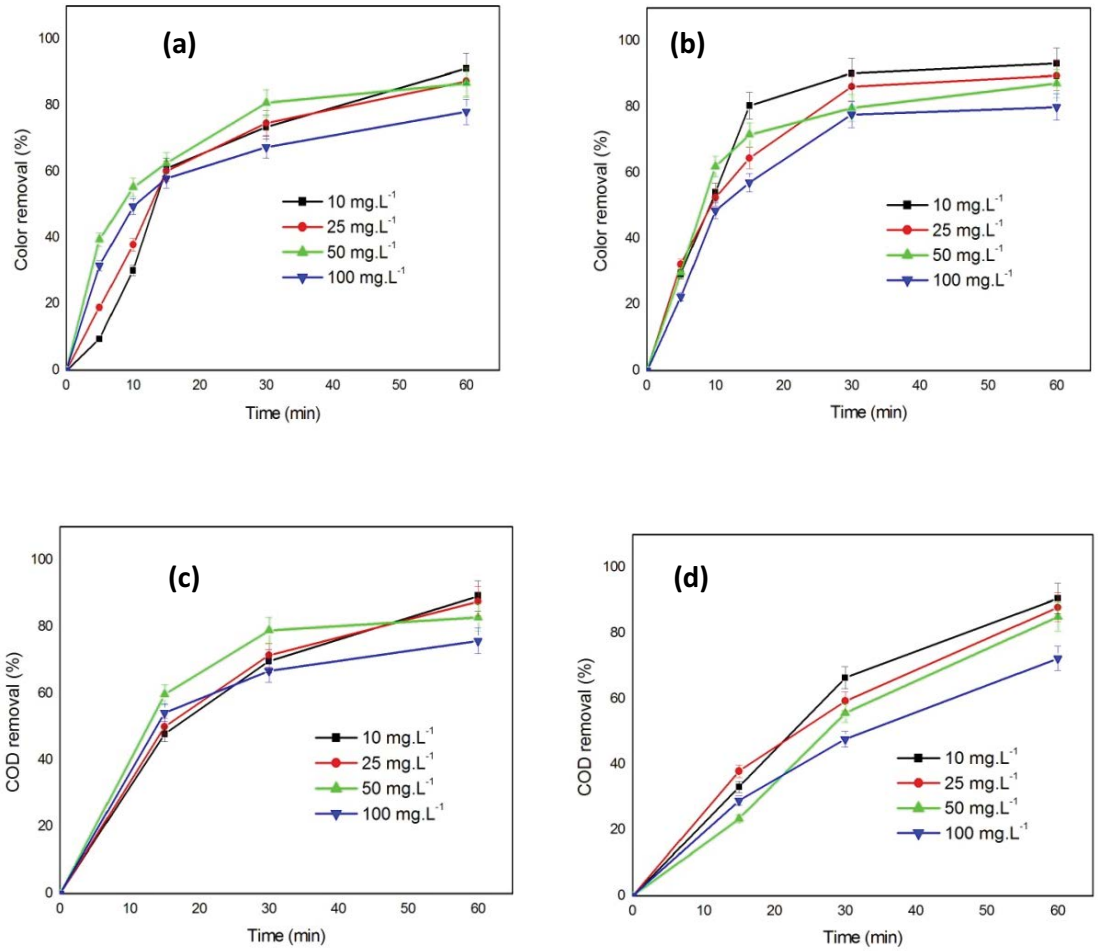

Fig. 6. Effect of Eriochrome Black T concentration on color (a) pyrite, (b) conv. catalyst and chemical oxygen demand (c) pyrite and (d) conv. catalyst removal of Eriochrome Black T solution ([pyrite] = 0.03 g·L^{-1}; [$FeSO_4$] = 0.038 g·L^{-1}; pH = 3; [Na_2SO_4] = 8 × 10^{-3} M; i = 15 mA·cm^{-2}; V = 200 mL).

recorded (Fig. 7c). The optimum pyrite dose is 0.03 g·L^{-1}. On the other hand, a similar trend of discoloration and mineralization of the Eriochrome Black T solution was observed with the conventional catalyst (Fig. 7b and d). Thus, 2.5 × 10^{-4} M $FeSO_4$ is an optimum concentration for discoloration and mineralization of the Eriochrome Black T solution by $FeSO_4$-EF. It is to be noted that for the two processes pyrite-EF and $FeSO_4$-EF, the concentration of iron has a significant effect on efficiency.

The decrease in effectiveness from a certain dose of pyrite or $FeSO_4$ can be explained by the excess of iron species (Fe^{2+} and Fe^{3+}). Indeed, the excess of Fe^{2+} accentuates the trapping of hydroxyl radicals [Eq. (4)] [41]. On the other hand, the excess of Fe^{3+} ions formed consumes hydrogen peroxide [30,31].

$$Fe^{2+} + {}^{\bullet}OH \rightarrow Fe^{3+} + OH^{-} \quad (4)$$

3.2.5. Effect of supporting electrolyte concentration

The presence of an electrolyte in a solution improves its conductivity and accelerates the transfer of electrons, which promotes the electro-Fenton reaction. Therefore, for low conductivity solutions, the addition of a supporting electrolyte is essential. In EF process, sodium sulfate is commonly used as the supporting electrolyte [42]. However, there is no unanimity on its optimal concentration. It seems that each system has its own optimal concentration of supporting electrolyte. In order to investigate the effect of the supporting electrolyte concentration on the degradation efficiency of EBT, pyrite-EF and $FeSO_4$-EF experiments were conducted at different Na_2SO_4 concentrations in the range of 4 × 10^{-3} to 3.5 × 10^{-2} M.

The results obtained show that when the concentration of the supporting electrolyte is increased from 4 × 10^{-3} to 8 × 10^{-3} M, the color removal efficiency increases from 83% to 90% for pyrite-EF (Fig. 8a) and from 84% to 93% for $FeSO_4$-EF (Fig. 8b). However, increasing the concentration from 8 × 10^{-3} to 3.5 × 10^{-2} M leads to a regression in color removal to 82.5% and 88% for pyrite-EF and $FeSO_4$-EF, respectively. The effect of the supporting electrolyte concentration on the solution mineralization observed with the pyrite (Fig. 8c) and $FeSO_4$ (Fig. 8d) catalysts was found to be identical to that of color removal. This result is logical

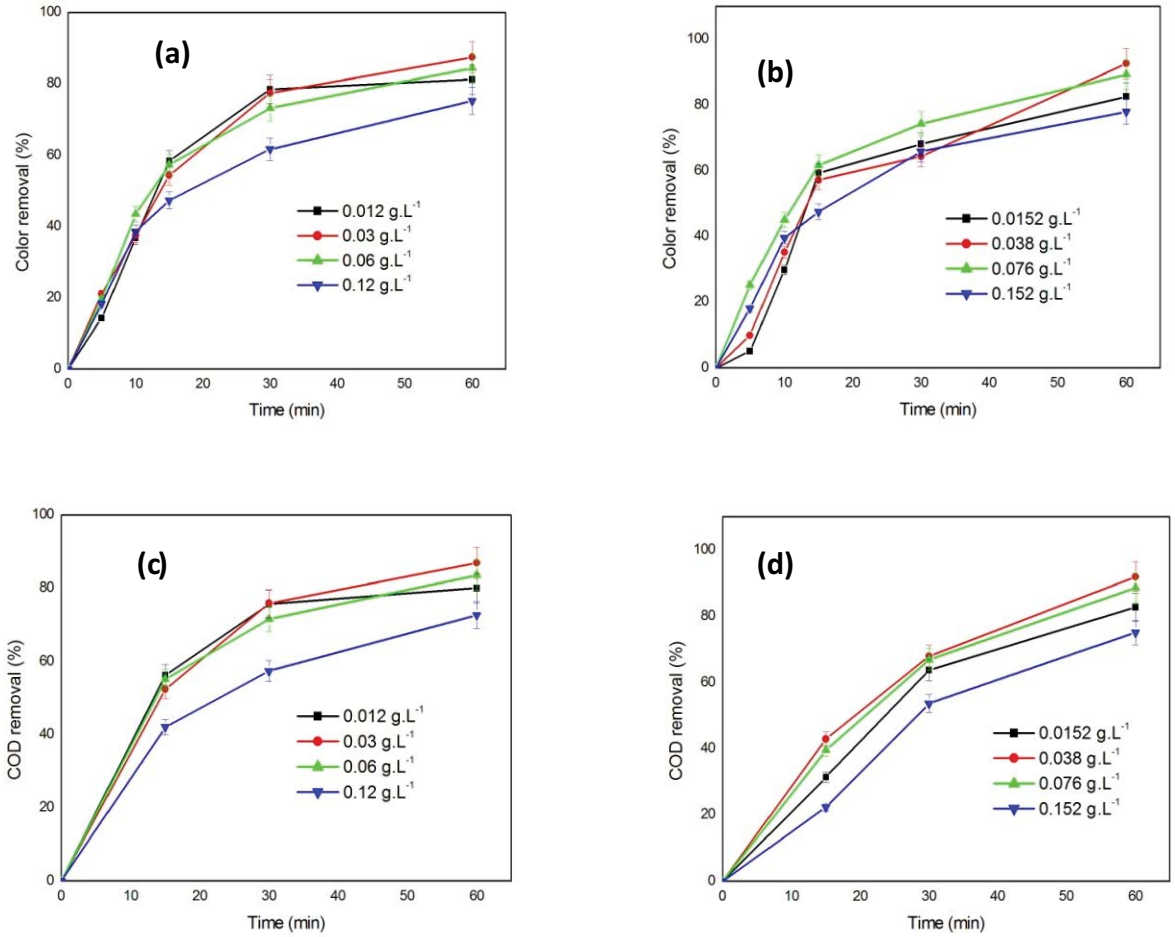

Fig. 7. Effect of the catalyst dose on color (a) pyrite, (b) conv. catalyst and chemical oxygen demand (c) pyrite and (d) conv. catalyst removal of Eriochrome Black T solution ([EBT] = 50 mg·L^{-1}; pH = 3; [Na_2SO_4] = 8 × 10^{-3} M; i = 15 mA·cm^{-2}; V = 200 mL).

since the mineralization of the solution is the final step in the degradation process. This result indicates that the effect of the supporting electrolyte concentration is independent of the catalyst nature.

The decrease in Eriochrome Black T removal efficiency resulting from increasing the Na_2SO_4 concentration from 8 × 10^{-3} to 3.5 × 10^{-2} M is probably due to the increased consumption of hydroxyl radicals by SO_4^{2-} ions in high concentrations [Eq. (5)] [40].

$$^{\bullet}OH + SO_4^{2-} \rightarrow OH^- + SO_4^{\bullet-} \quad (5)$$

3.2.6. Effect of current density

In order to investigate the effect of current density on the degradation of the EBT solution by pyrite-EF and $FeSO_4$-EF, some current values in the range of 5–35 mA·cm^{-2} were tested under the same operating conditions. The results reported in Fig. 9 show that for both natural (Fig. 9a and c) and conventional (Fig. 9b and d) catalysts, the rates of color (Fig. 9a and b) and COD (Fig. 9c and d) removal first increase as the current density increases from 5 to 15 mA·cm^{-2}, then decrease with increasing current density in the range 15–35 mA·cm^{-2}. This analysis shows that 15 mA·cm^{-2} is an optimal value for the current density. The decrease in Eriochrome Black T removal efficiency with current density in the range of 15–35 mA·cm^{-2} can be interpreted by the competitiveness of parasitic reactions with reactions 3, 4. Indeed, the increase in current density intensifies the hydrogen evolution at the cathode [Eq. (6)], the oxidation of Fe^{2+} to Fe^{3+} at the anode [Eq. (7)] and the oxidative/reductive decay of H_2O_2 at the anode [Eq. (8)] and cathode [Eq. (9)] [41,43].

$$2H^+ + 2e^- \rightarrow H_{2(g)} \quad (6)$$

$$Fe^{2+} \rightarrow Fe^{3+} + e^- \quad (7)$$

$$H_2O_2 + 2H^+ + 2e^- \rightarrow 2H_2O \quad (8)$$

$$H_2O_2 \rightarrow O_{2(g)} + 2H^+ + 2e^- \quad (9)$$

On the other hand, the results also revealed that the pyrite catalyst is as efficient as the conventional catalyst. For example, for the current density 15 mA·cm^{-2}, the color removal (86.75%) and the COD removal (82.86%) obtained with the natural catalyst (Fig. 9a and c) are slightly

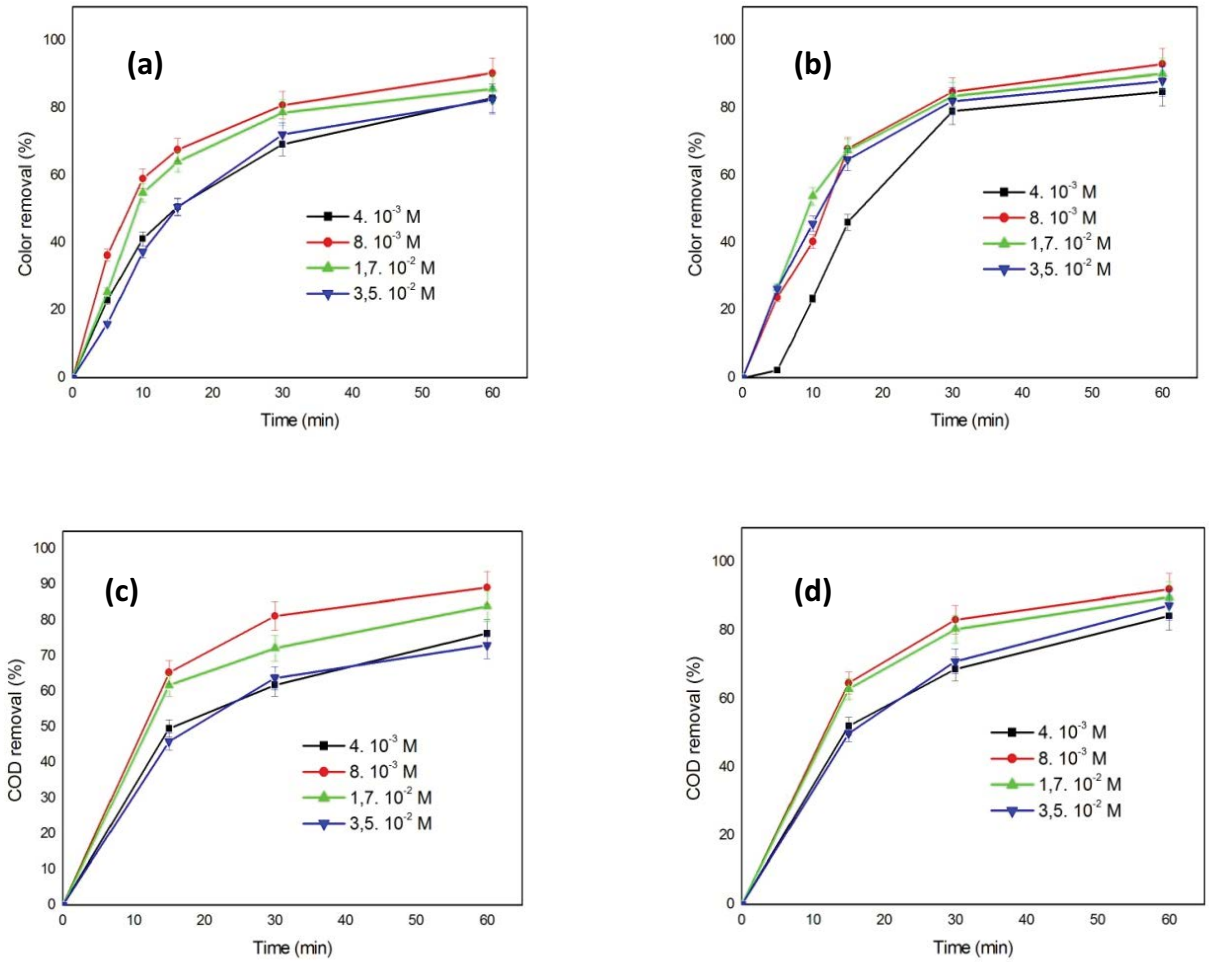

Fig. 8. Effect of supporting electrolyte concentration on color (a) pyrite, (b) conv. catalyst and chemical oxygen demand (c) pyrite and (d) conv. catalyst and chemical oxygen demand removal ([pyrite] = 0.03 g·L^{-1}; [$FeSO_4$] = 0.038 g·L^{-1}; [EBT] = 50 mg·L^{-1}; pH = 3; i = 15 mA·cm^{-2}; V = 200 mL).

lower than those obtained with the conventional catalyst (93.24%) and (91.97%) (Fig. 9b and d).

3.3. Kinetic analysis at optimal catalyst concentration

The rate constants k_1 and k_2 and the correlation coefficient R^2 calculated for the pseudo-first-order and pseudo-second-order kinetic models are shown in Table 6. The R^2 values clearly indicate that the pseudo-second-order model gives a better prediction than the pseudo-first-order model for EBT removal using pyrite as a natural catalyst. On the other hand, degradation of Eriochrome Black T using conventional catalyst follows the pseudo-first-order.

3.4. Energy consumption

The energy consumption (EC) (Table 7) in kWh·(g·COD)$^{-1}$ for the mineralization of the Eriochrome Black T solution using the two catalysts ($FeSO_4$ conv, FeS_2) under optimal conditions ([EBT] = 50 mg·L^{-1}; [pyrite] = 0.03 g·L^{-1}; [$FeSO_4$] = 0.038 g·L^{-1}; pH = 3; [Na_2SO_4] = 8 × 10^{-3} M; i = 15 mA·cm^{-2}; V = 200 mL) can be calculated according to the Eq. (10) [44]:

$$EC = \frac{IUt}{(\Delta COD)V_S} \quad (10)$$

where I: the applied current (A); U: cell voltage (V); t: electrolysis time (h); V_S: the solution volume (dm^3), and ΔCOD is the decrease in COD (g·dm^{-3}).

According to the results obtained (Table 7), it is noted that after 60 min of treatment by the EF process, the treatment with pyrite presents an energy consumption close to that of conventional catalyst, which shows that the heterogeneous-EF using pyrite as a catalyst is as effective as conventional homogeneous-EF using iron sulfate.

4. Conclusions

The discoloration and mineralization efficiency of the EBT solution by heterogeneous EF using natural catalysts (pyrite and hematite) was compared to that of homogeneous EF using the conventional catalyst ($FeSO_4$). Pyrite as a catalyst was found to be as effective as the $FeSO_4$ catalyst. It was also revealed that the effect of operating parameters on the efficiency of the pyrite-EF process showed a

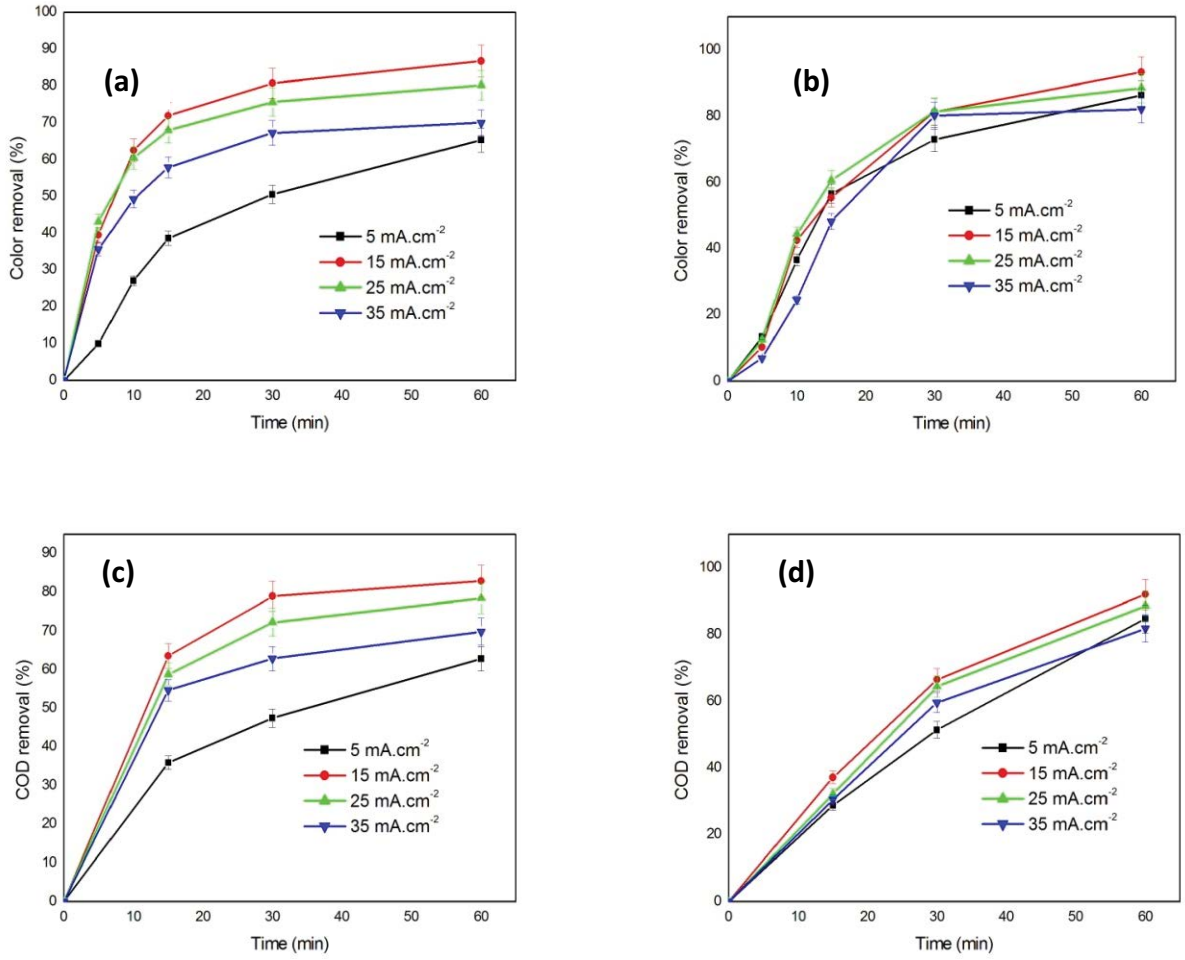

Fig. 9. Effect of current density on color (a) pyrite, (b) conv. catalyst and chemical oxygen demand removal (c) pyrite and (d) conv. catalyst of Eriochrome Black T solution ([EBT] = 50 mg·L^{-1}; [pyrite] = 0.03 g·L^{-1}; [$FeSO_4$] = 0.038 g·L^{-1}; pH = 3; [Na_2SO_4] = 8 × 10^{-3} M; V = 200 mL).

Table 6
Kinetic analysis at optimal catalyst concentration

Catalyst dose (g·L^{-1})	Pseudo-first-order		Pseudo-second-order	
	k_1 (min^{-1})	R^2	k_2 (M^{-1}·min^{-1})	R^2
[$FeSO_4$] = 0.03	0.0463	0.9840	0.4326	0.9602
[FeS_2] = 0.038	0.0361	0.9145	0.2961	0.9980

Table 7
Energy consumption

Catalyst	I (Å)	U (V)	Energy consumption (kWh·(g·COD)$^{-1}$)
$FeSO_4$	0.51	6.1	2.22
FeS_2	0.51	6.7	2.44

similar trend to that observed with the $FeSO_4$-EF process. Furthermore, the study of the effect of some operating parameters allowed determining the optimal conditions for the treatment of the Eriochrome Black T solution: 0.03 g·L^{-1} (pyrite dose), 8 × 10^{-3} M (supporting electrolyte concentration) and 15 mA·cm^{-2} (current density). This study demonstrated that natural pyrite could replace the conventional catalyst in the EF process.

References

[1] H. Zollinger, Coulour-Synthesis, Properties and Applications of Organic Dyes and Pigments, VCH Publishers, New York, 1987.
[2] S.J. Allen, K.Y.H. Khader, M. Bino, Electrooxidation of dyestuffs in waste waters, J. Chem. Technol. Biotechnol., 62 (1995) 111–117.
[3] R. Gong, Y. Sun, J. Chen, H. Liu, Ch. Yang, Effect of chemical modification on dye adsorption capacity of peanut hull, Dyes Pigm., 67 (2005) 175–181.
[4] K.-C. Chen, J.-Y. Wu, C.-C. Huang, Y.-M. Liang, Sz-C. John Hwang, Decolorization of azo dye using PVA-immobilized microorganisms, J. Biotechnol., 101 (2003) 241–252.
[5] C.A. Martínez-Huitle, E. Brillas, Decontamination of wastewaters containing synthetic organic dyes by electrochemical methods: a general review, Appl. Catal., B, 87 (2009) 105–145.
[6] S. Tsuda, N. Matsusaka, H. Madarame, The comet assay in eight mouse organs: result with 24 azo compounds, Mutat. Res., 465 (2000) 11–26.

[7] S. Hussain, N. Khan, S. Gul, S. Khan, H. Khan, Contamination of Water Resources by Food Dyes and Its Removal Technologies, M. Eyvaz, E. Yüksel, Ed., Water Chemistry, InTechOpen, 2019.
[8] M. Panizza, M.A. Oturan, Degradation of Alizarin Red by electro-Fenton process using a graphite-felt cathode, Electrochim. Acta, 56 (2011) 7084–7087.
[9] P.N. Dave, S. Kaur, E. Khosla, Removal of Eriochrome Black-T by adsorption on to eucalyptus bark using green technology, Indian J. Chem. Technol., 18 (2011) 53–60.
[10] Y. Men, Z. Li, L. Zhu, X. Wang, S. Cheng, Y. Lyu, New insights into membrane fouling during direct membrane filtration of municipal wastewater and fouling control with mechanical strategies, Sci. Total Environ., 896 (2023) 161775, doi: 10.1016/j.scitotenv.2023.161775.
[11] A.A. Owodunni, S. Ismail, S.B. Kurniawan, A. Ahmad, M.F. Imron, S.R. Sheikh Abdullah, A review on revolutionary technique for phosphate removal in wastewater using green coagulant, J. Water Process. Eng., 52 (2023) 103575, doi: 10.1016/j.jwpe.2023.103573.
[12] R. Xiao, T. Ou, S. Ding, Ch. Fang, Z. Xu, W Chu, Disinfection by-products as environmental contaminants of emerging concern: a review on their occurrence, fate and removal in the urban water cycle, Crit. Rev. Env. Sci. Technol., 53 (2023) 19–46.
[13] P. Shrivastava, M.K. Dwivedi, V. Malviya, P. Jain, A. Yadav, N. Jain, Adsorption of Crystal violet dye from aqueous solution by activated sewage treatment plant sludge, Desal. Water Treat., 283 (2023) 222–236.
[14] E. Brillas, C. Arias, P.-L. Cabot, F. Centellas, J.A. Garrido, R.M. Rodríguez, Degradation of organic contaminants by electrochemical oxidation methods, Port. Electrochem. Acta, 24 (2006) 159–189.
[15] E. Brillas, I. Sires, M. Oturan, Electro-Fenton process and related electrochemical technologies based on Fenton's reaction chemistry, Chem. Rev., 109 (2009) 6570–6631.
[16] M. Sánchez-Polo, J. López-Peñalver, G. Prados-Joya, M.A. Ferro-García, J. Rivera-Utrilla, Gamma irradiation of pharmaceutical compounds, nitroimidazoles, as a new alternative for water treatment, Water Res., 43 (2009) 4028–4036.
[17] I. Sirés, E. Brillas, Remediation of water pollution caused by pharmaceutical residues based on electrochemical separation and degradation technologies: a review, Environ. Int., 40 (2012) 212–229.
[18] J. Herny-Ramirez, F.M. Duarte, F.G. Martins, C.A. Costa, L.M. Madeira, Modelling of the synthetic dye Orange II degradation using Fenton's reagent: from batch to continuous reactor operation, Chem. Eng. J., 148 (2008) 394–404.
[19] E. Rosales, M. Pazos, M.A. Longo, M.A. Sanroman, Electro-Fenton decoloration of dyes in a continuous reactor: a promising technology in colored wastewater treatment, Chem. Eng. J., 155 (2009) 62–67.
[20] M. Panizza, G. Cerisola, Electro-Fenton degradation of synthetic dyes, Water Res., 43 (2009) 339–344.
[21] M.M. Ghoneim, H.S. El-Desoky, N.M. Zidan, Electro-Fenton oxidation of Sunset Yellow FCF azo-dye in aqueous solutions, Desalination, 274 (2011) 22–30.
[22] T.X. Huong Le, C. Charmette, M. Bechelany, M. Cretin, Facile preparation of porous carbon cathode to eliminate paracetamol in aqueous medium using electro-Fenton system, Electrochim. Acta, 188 (2016) 378–384.
[23] A. Dirany, I. Sires, N. Oturan, M.A. Oturan, Electrochemical abatement of the antibiotic sulfamethoxazole from water, Chemosphere, 81 (2010) 594–602.
[24] A.L. Estrada, Y.Y. Li, A. Wang, Biodegradability enhancement of wastewater containing cefalexin by means of the electro-Fenton oxidation process, J. Hazard. Mater., 227–228 (2012) 41–48.
[25] A. Özcan, Y. Şahin, M.A. Oturan, Complete removal of the insecticide azinphosmethyl from water by the electro-Fenton method – a kinetic and mechanistic study, Water Res., 47 (2013) 1470–1479.
[26] H. Belbel, R. Delimi, Z. Benredjem, T. Tayebi, Use of metallurgical waste as a catalyst in electro-Fenton process for degradation of dyes from aqueous solution, Desal. Water Treat., 273 (2022) 261–269.
[27] S. Bae, K. Dongwook, L. Woojin, Degradation of diclofenac by pyrite catalysed Fenton oxidation, Appl. Catal., B, 134–135 (2013) 93–102.
[28] N. Barhoumi, L. Labiadh, M.A. Oturan, N. Oturan, A. Gadri, S. Ammar, E. Brillas, Electrochemical mineralization of the antibiotic levofloxacin by electo-Fenton-pyrite process, Chemosphere, 141 (2015) 250–257.
[29] W.P. Kwan, B.M. Voelker, Rates of hydroxyl radical generation and organic compound oxidation in mineral-catalyzed Fenton-like systems, Environ. Sci. Technol., 37 (2003) 1150–1158.
[30] O. Ganzenko, N. Oturan, D. Huguenot, E.D. van Hullebusch, G. Esposito, M.A. Oturan Removal of psychoactive pharmaceutical caffeine from water by electro-Fenton process using BDD anode: effects of operating parameters on removal efficiency, Sep. Purif. Technol., 156 (2015) 987–995.
[31] A. Özcan, Y. Şahin, A.S. Koparal, M.A. Oturan, Carbon sponge as a new cathode material for the electro-Fenton process: comparison with carbon felt cathode and application to degradation of synthetic dye Basic Blue 3 in aqueous medium, J. Electroanal. Chem., 616 (2008) 71–78.
[32] B. Hou, H. Han, S. Jia, H. Zhuang, P. Xu, D. Wang, Heterogeneous electro-Fenton oxidation of catechol catalyzed by nano-Fe_3O_4: kinetics with the Fermi's equation, J. Taiwan Inst. Chem. Eng., 56 (2015) 138–147.
[33] P. Nazari, N. Askari, S.R. Setayesh, Oxidation-precipitation of magnetic Fe_3O_4/AC nanocomposite as a heterogeneous catalyst for electro-Fenton treatment, Chem. Eng. Commun., 207 (2020) 665–675.
[34] Q. Tian, F. Xiao, H. Zhao, X. Fei, X. Shen, G. Postole, G. Zhao, Simultaneously accelerating the regeneration of Fe^{II} and the selectivity of $2e^-$ oxygen reduction over sulfide iron-based carbon aerogel in electro-Fenton system, Appl. Catal., B, 272 (2020) 119039, doi: 10.1016/j.apcatb.2020.119039.
[35] E. Expósito, C.M. Sánchez-Sánchez, V. Montiel, Mineral iron oxides as iron source in electro-Fenton and photoelectro-Fenton mineralization processes, J. Electrochem. Soc., 154 (2007) 116–122.
[36] S.O. Ganiyu, M. Zhou, C.A. Martínez-Huitle, Heterogeneous electro-Fenton and photoelectro-Fenton processes: a critical review of fundamental principles and application for water/wastewater treatment, Appl. Catal., B, 235 (2018) 103–129.
[37] K. Barbari, R. Delimi, Z. Benredjem, S. Saaidia, A. Djemel, T. Chouchane, N. Oturan, M.A. Oturan, Photocatalycally-assisted electrooxidation of herbicide fenuron using a new bifunctional electrode PbO_2/SnO_2-Sb_2O_3/Ti//Ti/TiO_2, Chemosphere, 203 (2018) 1–10.
[38] M. Diagne, N. Oturan, M.A. Oturan, Removal of methyl parathion from water by electrochemically generated Fenton's reagent, Chemosphere, 66 (2007) 841–848.
[39] N. Oturan, M.A. Oturan, Chapter 8 – Electro-Fenton Process: Background, New Developments, and Applications, C.A. Martínez-Huitle, M.A. Rodrigo, O. Scialdone, Eds., Electrochemical Water and Wastewater Treatment, Butterworth-Heinemann, 2018, pp. 193–221.
[40] S. Saaidia, R. Delimi, Z. Benredjem, A. Mehellou, A. Djemel, K. Barbari, Use of a PbO_2 electrode of a lead-acid battery for the electrochemical degradation of methylene blue, Sep. Sci. Technol., 52 (2017) 1602–1614.
[41] M.F. Murrieta, E. Brillas, J.L. Nava, I. Sirés, Photo-assisted electrochemical production of HClO and Fe^{2+} as Fenton-like reagents in chloride media for sulfamethoxazole degradation, Sep. Purif. Technol., 250 (2020) 117236, doi: 10.1016/j.seppur.2020.117236.
[42] P.V. Nidheesh, R. Gandhimathi, Trends in electro-Fenton process for water and wastewater treatment: an overview, Desalination, 299 (2012) 1–15.
[43] H. Zazou, N. Oturan, H. Zhang, M. Hamdani, M.A. Oturan, Comparative study of electrochemical oxidation of herbicide 2,4,5-T: kinetics, parametric optimization and mineralization pathway, Sustainable Environ. Res., 27 (2017) 15–23.
[44] E. Brillas, C. Martínez-Huitle, Decontamination of wastewaters containing synthetic organic dyes by electrochemical methods. An updated review, Appl. Catal., B, 166–167 (2015) 603–643.